LETTERS

Pinning quantum phase transition for a Luttinger liquid of strongly interacting bosons

Elmar Haller[1], Russell Hart[1], Manfred J. Mark[1], Johann G. Danzl[1], Lukas Reichsöllner[1], Mattias Gustavsson[1], Marcello Dalmonte[2,3,4,5], Guido Pupillo[2,3] & Hanns-Christoph Nägerl[1]

Quantum many-body systems can have phase transitions[1] even at zero temperature; fluctuations arising from Heisenberg's uncertainty principle, as opposed to thermal effects, drive the system from one phase to another. Typically, during the transition the relative strength of two competing terms in the system's Hamiltonian changes across a finite critical value. A well-known example is the Mott–Hubbard quantum phase transition from a superfluid to an insulating phase[2,3], which has been observed for weakly interacting bosonic atomic gases. However, for strongly interacting quantum systems confined to lower-dimensional geometry, a novel type[4,5] of quantum phase transition may be induced and driven by an arbitrarily weak perturbation to the Hamiltonian. Here we observe such an effect—the sine–Gordon quantum phase transition from a superfluid Luttinger liquid to a Mott insulator[6,7]—in a one-dimensional quantum gas of bosonic caesium atoms with tunable interactions. For sufficiently strong interactions, the transition is induced by adding an arbitrarily weak optical lattice commensurate with the atomic granularity, which leads to immediate pinning of the atoms. We map out the phase diagram and find that our measurements in the strongly interacting regime agree well with a quantum field description based on the exactly solvable sine–Gordon model[8]. We trace the phase boundary all the way to the weakly interacting regime, where we find good agreement with the predictions of the one-dimensional Bose–Hubbard model. Our results open up the experimental study of quantum phase transitions, criticality and transport phenomena beyond Hubbard-type models in the context of ultracold gases.

Ultracold atomic gases are a versatile tunable laboratory system for the investigation of complex many-body quantum phenomena[9]. The study of quantum phases and quantum phase transitions is greatly enriched by the possibility of independently controlling the kinetic energy and the interactions. In deep optical-lattice potentials, the many-body dynamics of a weakly interacting gas is, to a very good approximation, governed microscopically by a Hubbard Hamiltonian[2] with a local on-site interaction energy U and kinetic energy J, which corresponds to tunnelling of atoms from one lattice site to the next. Experiments with Bose–Einstein condensates (BECs) of rubidium atoms have demonstrated the quantum phase transition from a superfluid phase for large J to an insulating Mott–Hubbard phase[3]. The transition between these two phases was obtained by quenching J in a lattice of finite depth. Recent experiments with fermionic atoms have demonstrated the presence of a fermionic Mott–Hubbard insulating state[10,11], potentially opening the way to the study of high-temperature superconductivity in proximity of the Mott–Hubbard phase in two dimensions.

Although the focus in the study of quantum phase transitions in the context of ultracold atoms has so far been on Hubbard-type physics in the weakly interacting regime, new quantum phenomena occur in lower dimensions, where the effects of quantum fluctuations and correlations are enhanced. In a one-dimensional (1D) bosonic gas, strong repulsive interactions lead to the formation of a Tonks–Girardeau gas, where bosons minimize their interaction energy by avoiding spatial overlap and acquire fermionic properties[12–15]. The addition of an arbitrarily weak lattice potential commensurate with the atomic density, that is, $n \approx 2/\lambda$, where n is the 1D density and $\lambda/2$ is the lattice periodicity, is expected to lead to an unusual type of quantum phase transition[4,6]: the strongly correlated 1D gas is immediately pinned by the lattice and the superfluid Tonks–Girardeau phase is turned into an insulating, gapped phase. Figure 1 contrasts the Hubbard-type superfluid-to-Mott-insulator transition with this pinning transition. Given the universality of 1D quantum physics, the pinning transition will occur for interacting bosons as well as for fermions in one dimension and has been discussed with respect to a variety of quantum models in low dimensions[4].

The pinning transition is described by the (1 + 1) quantum sine–Gordon model, which is an exactly solvable quantum field theory extensively studied in high-energy, condensed-matter and mathematical physics[5]. The sine–Gordon Hamiltonian reads

$$\mathcal{H} = \frac{\hbar v_s}{2\pi} \int \mathrm{d}x \left[(\partial_x \theta)^2 + (\partial_x \phi)^2 + \mathcal{V} \cos\left(\sqrt{4K}\theta \right) \right] \qquad (1)$$

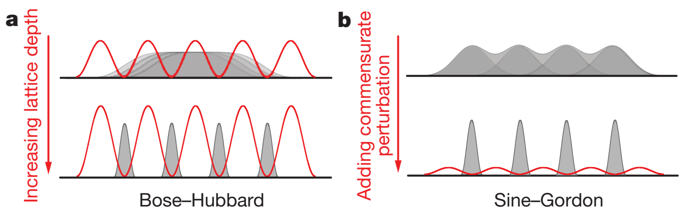

Figure 1 | Comparing two types of superfluid-to-Mott-insulator phase transition in one dimension. Schematic density distributions (grey) in the presence of a periodic potential (red solid line). **a**, Mott–Hubbard-type quantum phase transition for weak interactions[3]. The system is still superfluid at finite lattice depth (top). The transition to the insulating state is induced by increasing the lattice depth above a finite critical value (bottom). **b**, Sine–Gordon-type quantum phase transition for strong interactions[6]. In the absence of any perturbation, the system is a strongly correlated superfluid (top). For sufficiently strong interactions, not necessarily infinitely strong, an arbitrarily weak perturbation by a lattice potential commensurate with the system's granularity induces the transition to the insulating Mott state (bottom).

[1]Institut für Experimentalphysik und Zentrum für Quantenphysik, Universität Innsbruck, Technikerstraße 25, A–6020 Innsbruck, Austria. [2]Institut für Theoretische Physik, Universität Innsbruck, Technikerstraße 25, A–6020 Innsbruck, Austria. [3]Institut für Quantenoptik und Quanteninformation der Österreichischen Akademie der Wissenschaften, Technikerstraße 21a, A–6020 Innsbruck, Austria. [4]Dipartimento di Fisica dell'Università di Bologna, Via Irnerio 46, 40127 Bologna, Italy. [5]Istituto Nazionale di Fisica Nucleare, Via Irnerio 46, 40127 Bologna, Italy.

Here, $\partial_x\theta$ and $\partial_x\phi$ are respectively the fluctuations of the long-wavelength density field (θ) and phase field (ϕ) of the hydrodynamic description of the 1D liquid, with commutation relation $[\partial_x\theta(x), \phi(y)] = i\pi\delta(x-y)$, v_s is the velocity of the sound-like excitations of the 1D gas; $\mathcal{V} = Vn\pi/(\hbar v_s)$ is proportional to the depth, V, of a weak lattice[4,6]; δ is the delta-function; and $\hbar$ is Planck's constant, h, divided by 2π. For vanishing lattice ($\mathcal{V}=0$), equation (1) describes a Luttinger liquid, where the strength of interactions is parameterized by the dimensionless parameter $K = \hbar n\pi/(mv_s)$, which determines the long-distance power-law decay of the correlation functions; for example

$$\langle n(x)n(x')\rangle \approx n^2 + \frac{cK}{(x-x')^2} + \frac{c'\cos(2\pi n(x-x'))}{(x-x')^{2K}} + \cdots$$

with c and c' constants and m the atomic mass. The sine–Gordon model with a weak but finite lattice predicts a quantum phase transition of the Berezinskii–Kosterlitz–Thouless type from a superfluid state for $K > K_c = 2$, where the shallow lattice is an irrelevant perturbation, to an insulating Mott phase for $K < K_c$, for which the spectrum is gapped for any value of $\mathcal{V}$.

Although K is in general a phenomenological parameter, in the case of a 1D bosonic gas it can be microscopically related to the Lieb–Liniger parameter, $\gamma = mg/(\hbar^2 n)$, which characterizes interactions in a homogenous 1D system[16] (Methods). Here $g \approx 2\hbar\omega_\perp a_{3D}$ is the coupling constant of the Dirac delta-function interaction potential, $g\delta(x)$, where $\omega_\perp$ is the frequency of transverse confinement and a_{3D} is the three-dimensional (3D) scattering length. The strength of interactions and, thus, K can be tuned by varying a_{3D} near a Feshbach resonance[17]. The Tonks–Girardeau regime corresponds to $\gamma \gg 1$. Using the relation between K and γ, it has been shown[6] that particles are pinned for experimentally accessible values of $\gamma > \gamma_c \approx 3.5$ in the limit of a vanishingly weak lattice.

The pinning transition is expected to transform continuously into the Mott–Hubbard-type quantum phase transition, which occurs for the weakly interacting gas when the lattice depth becomes sufficiently large. Here, using a quantum gas of caesium atoms with tunable interactions confined to an array of independent 1D tubes (Methods), we drive the superfluid-to-Mott-insulator phase transition by varying γ, and determine the phase boundary all the way from the strongly to the weakly interacting regime using modulation spectroscopy and measurement of transport. For shallow lattices under conditions of commensurability, we observe immediate pinning of the particles for strong interactions when $\gamma > \gamma_c$.

We first discuss our experiments in the strongly interacting regime. We start with a 3D BEC of typically 1.3×10^5 caesium atoms without a detectable thermal fraction in a crossed-beam dipole trap with magnetic levitation[18], and initialize our system by creating a conventional 3D Mott–Hubbard state in a deep 3D lattice at $U/(6J) \approx 75$ with precisely one atom per lattice site[3]. We find, by reversing the loading, that the procedure does not lead to heating of the sample. The array of 1D tubes is obtained by reducing the lattice depth, V, in one direction. Our procedure ensures that a majority of tubes has a near-commensurate number density (Methods). A Feshbach resonance allows us to control a_{3D} with a precision of $3a_0$ (a_0, Bohr radius) that is limited by the presence of the magnetic field gradient. For the shallow lattice, we probe the state of the system by amplitude modulation spectroscopy[19,20]. We determine the presence of an excitation gap, E_g, by testing whether energy can be deposited into the 1D system at a given excitation frequency, f. We modulate V at f by 25–45% for 40–60 ms. After ramping down the lattice beams adiabatically with respect to the lattice band structure, and after a levitated expansion time of 40–60 ms (ref. 18), we detect the atoms by time-of-flight absorption imaging. We determine the spatial width of the atomic

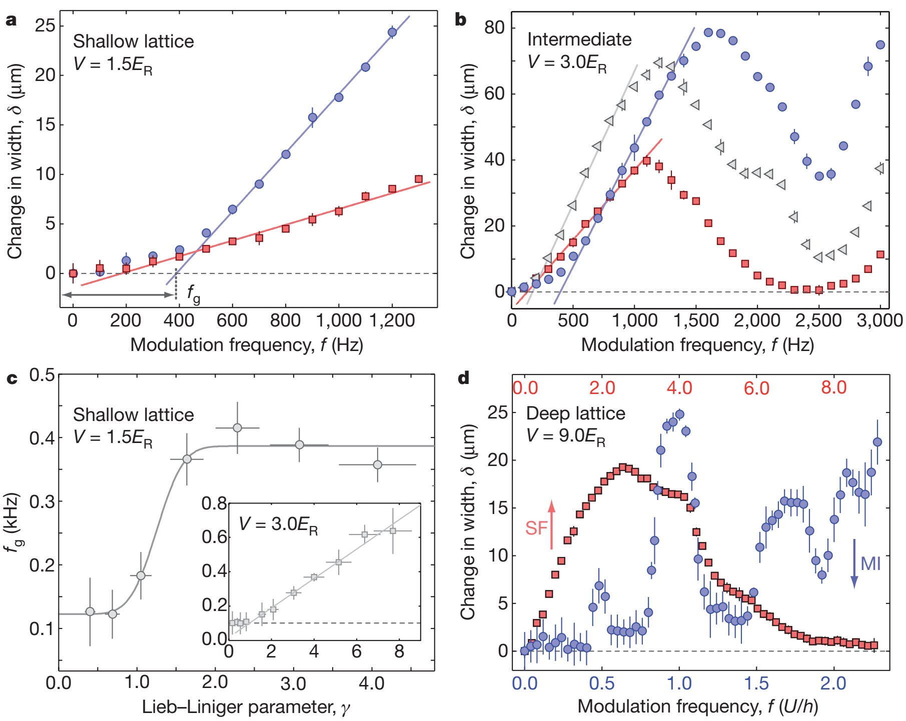

Figure 2 | Modulation spectroscopy on bosons in one dimension. **a**, **b**, **d**, Excitation spectra for low (**a**), intermediate (**b**), and high (**d**) lattice depth, V. The change, δ, in the spatial width after amplitude modulation is plotted as a function of the modulation frequency, f, for different values of γ. **a**, Characteristic spectra for $V = 1.5(1)E_R$ in the superfluid (squares: $a_{3D} = 115(2)a_0$, $\gamma = 1.0(1)$) and in the Mott regime (circles: $a_{3D} = 261(2)a_0$, $\gamma = 3.1(2)$). The solid lines are linear fits to the high-frequency parts of the spectra. We determine the axis intercepts, f_g, as indicated. **b**, Spectra for $V = 3.0(2)E_R$. The system is superfluid for $\gamma = 0.51(6)$ (squares) and exhibits a gap for $\gamma = 1.6(1)$ (triangles) and $\gamma = 4.1(3)$ (circles). **c**, Determination of the transition point for the case of the shallow lattice with $V = 1.5(1)E_R$. The frequency f_g is plotted as a function of γ. The solid line is an error-function fit to the data. Inset, f_g as a function of γ for $V = 3.0(2)E_R$. **d**, Spectra for $V = 9.0(5)E_R$ for weak (squares: $\gamma = 0.10(3)$) and strong (circles: $\gamma = 8.1(4)$) interactions in the superfluid (SF) and Mott-insulator (MI) regimes. Here we plot f in units of U/h. Modulation parameters and error bars are discussed in Methods.

sample from a Gaussian fit to the absorption profile and obtain the change, δ, in the spatial width relative to the unmodulated case as a function of f.

Two typical measurements are shown in Fig. 2a, one in the superfluid phase and one deep in the 1D Mott phase at the same lattice depth, $V = 1.5(1)E_R$, where $E_R = h^2/(2m\lambda^2)$ is the photon recoil energy. For weak interactions, the system exhibits a linear increase for δ as a function of f, which we attribute to the superfluid character of the gas. For strong interactions, the increase, after a slow rise, shows a clear kink. We attribute the initial slow rise to excitation of residual superfluid portions of our inhomogeneous system, and the sudden change in slope to the presence of an excitation gap. We associate f_g, the axis intercept obtained from a linear fit to the steep part of the spectrum, with the frequency of the gap. To determine the phase transition from the 1D Mott state to the superfluid state, we repeat this measurement for a given lattice depth as we scan γ by changing a_{3D}. A typical result is shown in Fig. 2c. The gap closes as γ is reduced. For values $V \leq 2.0E_R$, the transition point is identified with an abrupt step in f_g; that is, we determine the critical value, $\gamma_{c,V}$, at which the transition occurs using an error-function fit to the data. We always observe some small residual value for f_g, of about 120 Hz, for weak interactions. In general, we find that the measured value for the frequency of the gap is robust against variations in modulation amplitude, and that the slope increases with stronger modulation.

For comparison, in Fig. 2b, d we present excitation spectra for an intermediate value of the lattice depth and for the case of a deep lattice, respectively. For $V = 3.0(2)E_R$, the spectrum shows additional structure for high frequencies as band structure comes into play. We find that for $V > 2.0E_R$, the gap opens up approximately linearly as a function of γ beyond the critical value $\gamma_{c,V}$ (Fig. 2c, inset). For deep lattices and for comparatively weak interactions, the spectrum has a broad distribution characteristic of a superfluid. For stronger interactions, we recover the discrete excitation spectrum of the Mott phase in the Hubbard regime[3,19], with a pronounced peak at $f = 1.0U/h$. Additional peaks[21] can be found at $f = 0.5U/h$ and above $f = 1.5U/h$.

For the case of a deep lattice, we find that the state of the system is very sensitively probed by transport measurements[22,23]. A characteristic property of the Mott state is the inhibition of particle motion. In our experiment, with the capability to tune interactions we expect the phase transition to manifest itself, at fixed V, through a strong suppression of transport when the strength of the interaction is increased above a certain critical value. Essentially, we test whether momentum can be imparted to the 1D system as a function of interaction strength. For a given V, we apply a weak axial magnetic force for a short time to the interacting system, chosen such that the imparted momentum would be approximately $0.2\hbar k$, with $k = 2\pi/\lambda$, if the system were non-interacting. Then, as a function of a_{3D}, we determine the centre-of-mass displacement, x_0, of the sample after a fixed time of flight. Figure 3 shows that x_0 decreases monotonically with a_{3D}. For the case of a deep lattice with $V = 9.0(5)E_R$, the quenching of transport is abrupt. At a certain critical value of a_{3D}, transport is fully inhibited[24,25]. We find the critical a_{3D} value from a linear fit to the decreasing data and by determining the axis intercept, and derive from this the critical value $\gamma_{c,V}$. Reducing the lattice depth to $V = 5.0(3)E_R$ and $V = 2.0(1)E_R$ leads to a less abrupt quenching of transport. For stronger interactions, the decrease starts to level off. Nevertheless, the initial decrease is still linear, allowing us to determine $\gamma_{c,V}$ from an extrapolation to zero of the initially linear decrease. The inset in Fig. 3 shows the measured critical ratio, $(U/J)_c$, determined by our transport method as a function of lattice depth, V. When we compare our results with the predicted value[26], of $(U/J)_c \approx 3.85$, for the transition in one dimension, we find a slight systematic overestimation of the transition point. This, however, is expected in view of, for example, the spatial inhomogeneity of the sample and the Berezinskii–Kosterlitz–Thouless-type nature of the transition in a finite-size system.

We summarize our results in Fig. 4, where we present the phase diagram as a function of $1/\gamma$ and V. The set $\{\gamma_{c,V}\}$ defines the phase boundary between the 1D Mott insulator and the 1D superfluid. The measurements based on modulation spectroscopy cover a range from $V = 4E_R$ down to $0.5E_R$ (circles), and the transport measurements extend from $V = 2E_R$ to $10E_R$ (squares). In the weakly interacting regime, where $1/\gamma > 2$, our data are in good agreement with the prediction of the Mott–Hubbard model (dashed line). In the strongly interacting regime, where $1/\gamma < 1$, the measured phase boundary extrapolates to a finite critical value, $1/\gamma_c$, for the Lieb–Liniger parameter as the lattice depth is reduced to zero. Our results are in excellent quantitative agreement with the theory for a commensurate system based on the sine–Gordon model (solid line; see Methods), for which $\gamma_c = 3.5$. We also find good agreement between our two

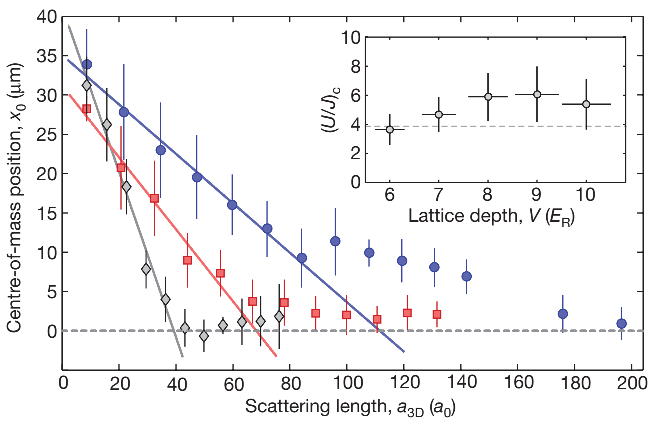

Figure 3 | Transport measurements on the 1D Bose gas. Centre-of-mass displacement, x_0, as a function of a_{3D} for $V = 9.0(5)E_R$ (diamonds), $V = 5.0(3)E_R$ (squares) and $V = 2.0(1)E_R$ (circles). We extrapolate the linear slope at small values of a_{3D} and associate the transition point with the axis intercept. For the data with $V = 2.0(1)E_R$, transport is not fully quenched as the condition of commensurability is not fulfilled for all atoms. All errors are the 1σ statistical error. Inset, the measured critical ratio $(U/J)_c$ at the transition point as a function of lattice depth, V. The dashed line indicates the theoretical result, $(U/J)_c \approx 3.85$, in the 1D Bose–Hubbard regime[26].

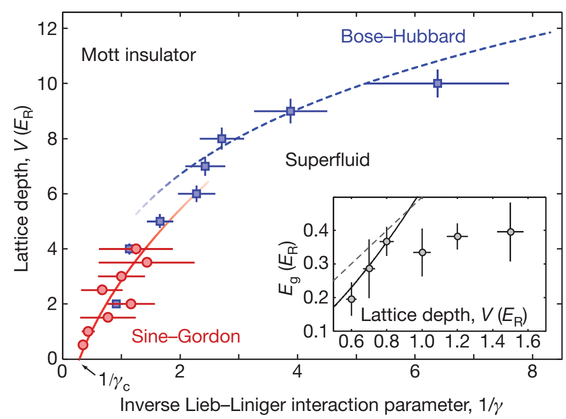

Figure 4 | Phase diagram for the strongly interacting 1D Bose gas. The plane of inverse Lieb–Liniger interaction parameter, $1/\gamma$, and optical lattice depth, V (in units of E_R), showing the superfluid and Mott-insulating phases in one dimension. The critical interaction parameter is γ_c. For strong interactions and shallow lattices, we determine the transition by amplitude modulation spectroscopy (circles). For weak interactions and deep lattices, we probe the phase boundary using transport measurements (squares). The solid and dashed lines are the predictions from the sine–Gordon and Bose–Hubbard models, respectively. Error bars are discussed in the Methods. Inset, the measured gap energy, $E_g = hf_g$, as a function of V for $\gamma = 11(1)$, and comparison between our data and the analytical result for finite γ as given by the sine–Gordon model (solid line; see Methods). Also shown is the universal behaviour, $E_g = V/2$, which is valid for non-interacting fermions (dashed line).

types of measurement technique in the intermediate regime ($V = 2E_R$–$4E_R$). Our results demonstrate the striking consequence of strong interactions in 1D geometry in the presence of a lattice: beyond a critical value, γ_c, an insulating Mott state exists for vanishingly small lattice depth. The particles are immediately pinned by the lattice.

We measure a finite gap energy, E_g, for $\gamma > \gamma_c$ in the regime of a shallow lattice. In the limit as $\gamma \to \infty$ and $V \to 0$, the simple relation $E_g = V/2$ is expected to hold because the bosonic system has become fully fermionized and the lattice effectively induces a band insulator of fermions[6]. In the inset in Fig. 4, we plot the measured E_g as a function of V at fixed $\gamma = 11(1)$. For $V < E_R$, our data are in good agreement with the analytical result for the gap energy at finite γ (Methods). We note that for $V \geq E_R$ we observe a deviation in E_g away from the predicted values. This deviation occurs for shallow lattices. However, the curve is expected to have a reduced slope for deeper lattices, for which E_g becomes of order U and is only weakly dependent on V.

Our results are a benchmark realization of quantum field theory models with tunable parameters in cold atomic systems. These results open up the experimental study of the out-of-equilibrium properties of sine–Gordon-type models. In particular, thermalization in integrable models beyond the Luttinger-liquid model, quenches across quantum phase transitions, and their relations to the breakdown of the adiabatic theorem in low dimensions can now be investigated with full tunability of system parameters.

METHODS SUMMARY

Sample preparation. We begin with a BEC, with no detectable thermal fraction, of typically 1.3×10^5 caesium atoms in the $|F = 3, m_F = 3\rangle$ hyperfine ground state in a crossed-beam dipole trap with magnetic levitation. Details of the BEC preparation are presented elsewhere[18]. The BEC is adiabatically transferred to the 3D lattice by exponentially ramping up the power in the lattice laser beams within 300 ms. We create a 3D Hubbard-type Mott insulator with precisely one atom per site in the central region of the trap by adjusting the external dipole-trap confinement before loading into the lattice. The array of vertically oriented tubes is created by ramping down the power in the vertically propagating beam pair. Typical trapping frequencies for the tubes are $\omega_r = 2\pi \times 12{,}300(200)$ Hz and $\omega_z = 2\pi \times 21.9(3)$ Hz along the transversal and longitudinal directions, respectively.

It is not necessary to strictly adhere to the commensurate density condition to observe the pinning transition for very weak lattices[6]. However, we prepare our sample such that the commensurability condition is on average best fulfilled over the inhomogeneously populated array of tubes. We find this optimal configuration when the total atom number is chosen such that the peak density of the centre tube is approximately $1.2n_c$, where $n_c = 2/\lambda$ is the commensurate 1D density. Typically there are about 60 atoms in the centre tube.

Phase transition line. For the case of a 1D Bose gas in a weak optical lattice, the effective sine–Gordon Hamiltonian (equation (1)) is realized. In this regime, the Berezinskii–Kosterlitz–Thouless transition line between the superfluid and the Mott-insulating phases can be derived in terms of V and $\gamma = \gamma_{c,V}$ as

$$\frac{V}{E_R} = 2\left(\frac{\pi}{\sqrt{\gamma - \gamma^{3/2}/(2\pi)}} - 2\right)$$

When the system is weakly interacting ($\gamma \ll 1$) and for deeper lattices ($V \gg E_R$), the system can be described by the Bose–Hubbard Hamiltonian[2]. In this regime, the quantum phase transition between a superfluid and a Mott–Hubbard state occurs at[26] $(U/J)_c \approx 3.85$, which determines a transition line in the V–γ plane according to

$$\frac{4V}{E_R} = \ln^2\left[\frac{2\sqrt{2}\pi}{\gamma}\left(\frac{U}{J}\right)_c \sqrt{\frac{V}{E_R}}\right]$$

Here J is the hopping energy and U is the on-site interaction energy of the Bose–Hubbard model.

Full Methods and any associated references are available in the online version of the paper at www.nature.com/nature.

Received 16 April; accepted 9 June 2010.

1. Sachdev, S. *Quantum Phase Transitions* (Cambridge Univ. Press, 2000).
2. Jaksch, D., Bruder, C., Cirac, J., Gardiner, C. & Zoller, P. Cold bosonic atoms in optical lattices. *Phys. Rev. Lett.* **81,** 3108–3111 (1998).
3. Greiner, M. *et al.* Quantum phase transition from a superfluid to a Mott insulator in a gas of ultracold atoms. *Nature* **415,** 39–44 (2002).
4. Giamarchi, T. *Quantum Physics in One Dimension* (Oxford Univ. Press, 2003).
5. Gogolin, A. O., Tsvelik, A. M. & Nersesyan, A. A. *Bosonization and Strongly Correlated Systems* (Cambridge Univ. Press, 1998).
6. Büchler, H. P., Blatter, G. & Zwerger, W. Commensurate-incommensurate transition of cold atoms in an optical lattice. *Phys. Rev. Lett.* **90,** 130401 (2003).
7. Pokrovsky, V. L. & Talapov, A. L. Ground state, spectrum, and phase diagram of two-dimensional incommensurate crystals. *Phys. Rev. Lett.* **42,** 65–67 (1979).
8. Coleman, S. Quantum sine-Gordon equation as the massive Thirring model. *Phys. Rev. D* **11,** 2088–2097 (1975).
9. Bloch, I., Dalibard, J. & Zwerger, W. Many-body physics with ultracold gases. *Rev. Mod. Phys.* **80,** 885–964 (2008).
10. Jördens, R., Strohmaier, N., Günter, K., Moritz, H. & Esslinger, T. A Mott insulator of fermionic atoms in an optical lattice. *Nature* **455,** 204–207 (2008).
11. Schneider, U. *et al.* Metallic and insulating phases of repulsively interacting fermions in a 3D optical lattice. *Science* **322,** 1520–1525 (2008).
12. Girardeau, M. Relationship between systems of impenetrable bosons and fermions in one dimension. *J. Math. Phys.* **1,** 516–523 (1960).
13. Paredes, B. *et al.* Tonks–Girardeau gas of ultracold atoms in an optical lattice. *Nature* **429,** 277–281 (2004).
14. Kinoshita, T., Wenger, T. & Weiss, D. S. Observation of a one-dimensional Tonks-Girardeau gas. *Science* **305,** 1125–1128 (2004).
15. Haller, E. *et al.* Realization of an excited, strongly correlated quantum gas phase. *Science* **325,** 1224–1227 (2009).
16. Lieb, E. H. & Liniger, W. Exact analysis of an interacting Bose gas. *Phys. Rev.* **130,** 1605–1616 (1963).
17. Chin, C., Grimm, R., Julienne, P. & Tiesinga, E. Feshbach resonances in ultracold gases. *Rev. Mod. Phys.* **82,** 1225–1286 (2010).
18. Kraemer, T. *et al.* Optimized production of a cesium Bose-Einstein condensate. *Appl. Phys. B* **79,** 1013–1019 (2004).
19. Stöferle, T., Moritz, H., Schori, C., Köhl, M. & Esslinger, T. Transition from a strongly interacting 1D superfluid to a Mott-insulator. *Phys. Rev. Lett.* **92,** 130403 (2004).
20. Iucci, A., Cazalilla, M. A., Ho, A. F. & Giamarchi, T. Energy absorption of a Bose gas in a periodically modulated optical lattice. *Phys. Rev. A* **73,** 041608(R) (2006).
21. Clark, S. R. & Jaksch, D. Signatures of the superfluid to Mott-insulator transition in the excitation spectrum of ultracold atoms. *N. J. Phys.* **8,** 160 (2005).
22. Mun, J. *et al.* Phase diagram for a Bose-Einstein condensate moving in an optical lattice. *Phys. Rev. Lett.* **99,** 150604 (2007).
23. Fertig, C. D. *et al.* Strongly inhibited transport of a degenerate 1D Bose gas in a lattice. *Phys. Rev. Lett.* **94,** 120403 (2005).
24. Altman, E., Polkovnikov, A., Demler, E., Halperin, B. I. & Lukin, M. D. Superfluid-insulator transition in a moving system of interacting bosons. *Phys. Rev. Lett.* **95,** 020402 (2005).
25. Schachenmayer, J., Pupillo, G. & Daley, A. J. Time-dependent currents of one-dimensional bosons in an optical lattice. *N. J. Phys.* **12,** 025014 (2010).
26. Rapsch, S., Schollwck, U. & Zwerger, W. Density matrix renormalization group for disordered bosons in one dimension. *Europhys. Lett.* **46,** 559–564 (1999).

Acknowledgements We thank W. Zwerger for discussions. We are indebted to R. Grimm for generous support. We gratefully acknowledge funding by the Austrian Ministry of Science and Research (Bundesministerium für Wissenschaft und Forschung) and the Austrian Science Fund (Fonds zur Förderung der wissenschaftlichen Forschung) in the form of a START prize grant, and by the European Union through the STREP FP7-ICT-2007-C project NAME-QUAM (Nanodesigning of Atomic and Molecular Quantum Matter) and within the framework of the EuroQUASAR collective research project QuDeGPM. R.H. is supported by a Marie Curie International Incoming Fellowship within the 7th European Community Framework Programme.

Author Contributions The experimental work was done by E.H., R.H., M.J.M., J.G.D, L.R., M.G. and H.-C.N. Theoretical analysis and support was provided by M.D. and G.P. The manuscript was written with substantial contributions from all authors.

Author Information Reprints and permissions information is available at www.nature.com/reprints. The authors declare no competing financial interests. Readers are welcome to comment on the online version of this article at www.nature.com/nature. Correspondence and requests for materials should be addressed to H.-C.N. (christoph.naegerl@uibk.ac.at).

METHODS

1D Bose gas in a weak optical lattice. In the absence of the optical lattice ($V=0$), the Luttinger-liquid parameter, K, can be expressed in terms of the Lieb–Liniger parameter, $\gamma = gm/(\hbar^2 n)$, for all strengths of interaction[16,27]. For $\gamma \leq 10$ and $\gamma \gg 10$, we find that $K \approx \pi/\sqrt{\gamma - \gamma^{3/2}/(2\pi)}$ and $K \approx (1+2/\gamma)^2$, respectively. The addition of a weak but finite commensurate optical lattice with $V \leq E_R$ realizes the effective sine–Gordon Hamiltonian (equation (1)). Using a perturbative renormalization group approach, the Berezinskii–Kosterlitz–Thouless transition line between the superfluid and the Mott-insulating phases can be derived in terms of V and $\gamma = \gamma_{c,V}$ as

$$\frac{V}{E_R} = 2\left(\frac{\pi}{\sqrt{\gamma - \gamma^{3/2}/(2\pi)}} - 2\right)$$

For small lattice depths, the integrable structure of the sine–Gordon model[28,29] allows the derivation of the following analytical expression for the dependence of the spectral gap, E_g, on V and K:

$$\frac{E_g}{E_R} = \frac{8\Gamma\left[\frac{\pi K}{2(2-K)}\right]}{\sqrt{\pi}\,\Gamma\left[\frac{2+K(\pi-1)}{2(2-K)}\right]}\left[\left(\frac{K^2 V}{16 E_R}\frac{\Gamma\left[1-\frac{K}{2}\right]}{\Gamma\left[1+\frac{K}{2}\right]}\right)\right]^{\frac{1}{2-K}}$$

Here Γ is the gamma function. For strong interactions ($K \approx 1$), the dependence of the gap on V is linear and E_g approaches the free fermion value, $E_g = V/2$. In the vicinity of $K = 2$, the gap closes exponentially approaching the Berezinskii–Kosterlitz–Thouless transition line.

Deep lattice: the Bose–Hubbard model. In the weakly interacting regime ($\gamma \ll 1$), for $V \gg E_R$, when all atoms occupy the lowest vibrational state in each potential well of the lattice, the system can be described by the following Bose–Hubbard model[2]:

$$H = -J\sum_i \left(b_i^\dagger b_{i+1} + \text{h.c.}\right) + \frac{U}{2}\sum_i b_i^\dagger b_i^\dagger b_i b_i$$

Here b_i and $b_i^\dagger$ are the operators respectively destroying and creating a bosonic particle at the position of the ith well, $J = 4E_R(V/E_R)^{3/4}/\sqrt{\pi}\exp(-2\sqrt{V/E_R})$ is the hopping energy and $U = \sqrt{2\pi}g(V/E_R)^{1/4}/\lambda$ is on-site interaction energy. The quantum phase transition between a superfluid and a Mott–Hubbard state occurs at[26] $(U/J)_c \approx 3.85$, which determines a transition line in the V–γ plane according to

$$\frac{4V}{E_R} = \ln^2\left[\frac{2\sqrt{2}\pi}{\gamma}\left(\frac{U}{J}\right)_c\sqrt{\frac{V}{E_R}}\right]$$

Magnetic Feshbach resonance. The strength of interaction can be tuned by means of a broad magnetic Feshbach resonance with a pole at -11.7 G and with a zero crossing for the scattering length near 17 G (ref. 18). To hold the atoms in the vertically oriented tubes, magnetic levitation by means of a magnetic field gradient is applied. For a caesium atom in the hyperfine state $|F=3, m_F=3\rangle$ a magnetic field gradient of 31.1 G cm^{-1} cancels the gravitational force.

Lattice loading and array of 1D tubes. We create a 3D optical lattice by interference of three pairs of counter-propagating dipole-trap laser beams at wavelength $\lambda = 1{,}064.5$ nm with $1/e^2$ beam waists of $\sim 350\,\mu$m. The atomic BEC, initially trapped in a crossed-beam dipole trap, is adiabatically transferred to the 3D lattice by exponentially ramping up the power in the lattice laser beams within 300 ms. At the same time, we increase the interaction strength by linearly increasing the magnetic field strength, and finally reach a 3D Hubbard-type Mott insulator with precisely one atom per site in the central region. The array of vertically oriented tubes is created by linearly ramping down the power in the vertically propagating beam pair in 100 ms, reaching lattice depths from $10E_R$ to $0.5E_R$. Simultaneously, we linearly reduce the magnetic field strength to set a_{3D}. Typical trapping frequencies for the tubes are $\omega_r = 2\pi \times 12{,}300(200)$ Hz and $\omega_z = 2\pi \times 21.9(3)$ Hz along the transversal and longitudinal directions, respectively. The depth of the lattice along the tubes is calibrated by the pulsed Raman–Nath technique[30]. The transversal trapping frequencies of the tubes are determined by parametric-heating measurements. The distribution of the atom number per tube can be directly determined from the density distribution in the Mott-insulating phase and shows an occupation of about 60 atoms in the centre tube. Here we assume a constant filling factor of one atom and no thermal or superfluid components. In view of our inhomogeneous system, we calculate γ for a given tube by assuming a 1D Thomas–Fermi distribution and taking the centre density. The reported γ value is a weighted average over all tubes.

Commensurability. To observe the pinning transition, it is not necessary to fulfil the condition of commensurability precisely[6]. A finite commensurability parameter, $Q = 2\pi(n - n_c)$, corresponds to a shift, $\delta\mu$, of the chemical potential, μ. Here $n_c = 2/\lambda$ is the commensurate 1D density. The system stays locked to the Mott-insulating phase as long as $\delta\mu$ remains smaller than the energy necessary to add another atom. When Q increases beyond a critical value, $Q_c(\gamma, V)$, the system develops finite-density excitations, which destroy the long-range order of the Mott insulator. We find that, for the array of 1D tubes, the commensurability condition in the superfluid regime is fulfilled best when the total atom number is chosen in such a way that the peak density of the centre tube is approximately $1.2n_c$.

Modulation parameters and error bars. For the data in Fig. 2a, b, d, we chose the following modulation times and amplitudes: 40 ms, 35% (Fig. 2a); 40 ms, 30% (Fig. 2b); 30 ms, 35% for the superfluid phase and 25% for the Mott phase (Fig. 2d). In Fig. 2a, b, d, the error bars for δ reflect the 1σ statistical error. In Fig. 2c, the error bars for f_g are derived from the 1σ error in the fit parameters. The error in γ results from the 1σ statistical error in the independent input variables and the spread of γ due to the distribution of tubes. For the data in Fig. 4, the error in γ is derived from the 1σ error in the fit parameters for the modulation measurements. For the transport measurements, the error in γ results from the 1σ statistical error in the independent input variables and the spread of γ due to the distribution of tubes. The error bars for V indicate the 1σ error from the calibration of the lattice depth.

27. Cazalilla, M. A. Bosonizing one-dimensional cold atomic gases. *J. Phys. B* **37**, S1–S47 (2004).
28. Zamolodchikov, A. B., &. Zamolodchikov, A. B. Factorized S-matrices in two dimensions as the exact solutions of certain relativistic quantum field theory models. *Ann. Phys.* **120**, 253–291 (1979).
29. Zamolodchikov, A. Mass scale in the sine-Gordon model and its reductions. *Int. J. Mod. Phys. A* **10**, 1125–1150 (1995).
30. Gould, P. L., Ruff, G. A. & Pritchard, D. E. Diffraction of atoms by light: the near-resonant Kapitza-Dirac effect. *Phys. Rev. Lett.* **56**, 827–830 (1986).